CHEMICAL ENGINEERING TRANSACTIONS
VOL. 77, 2019
A publication of AIDIC
The Italian Association of Chemical Engineering
Online at www.cetjournal.it
Guest Editors: Genserik Reniers, Bruno Fabiano

ISBN 978-88-95608-74-7; **ISSN** 2283-9216
DOI: 10.3303/CET1977062

Jet Fires and Reaction Runaway Interaction: a Multiscale Approach

Federico Florit, Simone Favrin, Renato Rota, Marco Derudi*

Politecnico di Milano, Dip. di Chimica, Materiali e Ingegneria Chimica "G. Natta", Via Mancinelli 7 - 20131 Milano – Italy
marco.derudi@polimi.it

In industrial safety, large engulfing jet fires can cause damages and collapse of process vessels with catastrophic consequences; however, even smaller jet fires can be extremely dangerous due to their ability to induce hazardous conditions when chemical reacting systems are involved.
This work investigates the ethoxylation of 1-dodecanol as a case-study to investigate the potentialities of a multiscale approach able to analyse scenarios of accidental impingement on a chemical reactor involving a jet fire.
In particular, the investigated system was a Venturi tower reactor, where the reacting fluid is pumped, cooled via an external heat exchanger and sprayed from the top of the reactor together with ethylene oxide. The aim is to understand if and when the cooling power of the external heat exchanger can prevent dangerous temperature build-up in the chemical reactor.
The multiscale approach used in this work involves a series of mathematical simulations aimed at evaluating the effects of different jet fires in terms of heat flux entering the Venturi reactor impinged by a jet fire. These simulations were carried out using a mathematical model developed in the framework of computational fluid dynamics (CFD). The results of such simulations were used to carry out a parametric study with a 0D model able to foresee the dynamic behaviour of the reactor impinged by the jet fire.
Preliminary results confirmed the possibility of linking jet fires characteristics with the time available before dangerous conditions in the Venturi reactor occur, therefore allowing for making an estimation of the time available for activating proper mitigation measures.

1. Background

Risk assessment is a complex process that requires interaction of multiple expertise and tools.
Among the others, Computational fluid dynamics (CFD) codes are a growing tool for risk analysis in the chemical process industry thanks to their ability in modelling several complex scenarios such as fires and dispersions (Chakrabarty et al., 2015; Tavelli et al., 2013; Tavelli et al., 2014). In principle, a CFD code could describe an accidental scenario on every scale (from the chemical reaction microscopic scale to the macroscopic scale of the environmental dispersion). However, such a multiscale approach is still unfeasible due to the high computational effort required. Therefore, simplified models, which adopt proper assumptions, are often employed to represent specific accidental scenarios such as runaway phenomena in mixed vessels that can be described with a zero-dimensional (0D) model, where time is the only independent variable. A hybrid approach, which is investigated in this paper involves the coupling of CFD and 0D models to obtain sound results using reasonable computational resources. In particular, a typical domino effect scenario involving a fire impingement of vessels (inside which a possibly runaway reaction occurs) is analysed in Reniers and Cozzani (2013) using a CFD tool to properly model the heat flux distribution on the vessel surface and a 0D model for investigating runaway scenarios in chemical reactor as consequence of a flame impingement.
The idea behind this approach is to obtain a comprehensive evaluation of the risk generated from a specific scenario, analysing the actual effects of a flame and providing a tool to support the design of safety barriers for domino effects.

Paper Received: 24 October 2018; Revised: 1 May 2019; Accepted: 22 June 2019

Please cite this article as: Florit F., Favrin S., Rota R., Derudi M., 2019, Jet Fires and Reaction Runaway Interaction: A Multiscale Approach, Chemical Engineering Transactions, 77, 367-372 DOI:10.3303/CET1977062

2. Materials and methods

Fire Dynamics Simulator (FDS) was selected as CFD program, being a common tool in fire protection engineering. FDS is an uncompressible Large Eddy Simulation solver created and distributed by National Institute of Standard and Technology (NIST). Peculiar characteristics of FDS are the use of an orthogonal grid and simplified model for the combustion. These features grant short computational time and consequently the possibility to study the dynamics of the fires. Even though the simplified assumption, FDS has an excellent heat transfer description, confirmed by the extensive validation performed (McGrattan et al., 2013).
Related to the present application, two aspects of FDS should be highlighted. First, FDS ability to describe the interaction between the flame and the geometry is the major advantage of this approach, because it allows to obtain a proper description of the area involved in the heat transfer process and the time variation in the thermal load. Second, FDS Heat transfer model in solid boundaries is a 1D Fourier equation. Both radiative and convective heat transfer are calculated. Convective heat transfer is computed using a combination of natural and forced convection correlations. The user has the possibility to change the constants of the model to suit particular scenarios; more detailed information can be found in McGrattan et al. (2013). Despite the limitation to incompressible flows, preliminary works in FDS suggest the possibility to model vertical jet fires properly (Sun et al, 2017, Favrin et al, 2018).
The adopted model for simulating runaway phenomena assumes well mixing in the analysed reaction vessel, making it a 0D model as usually done for runaway investigation (Maestri and Rota, 2016). When a chemical reactor is impinged by a jet fire, temperature increases and the reaction proceeds at a faster rate, further accelerating the temperature rise. Temperature increase acts indirectly on the vessel pressure, which ultimately causes the reactor rupture if safety devices are not properly designed and installed. Therefore, a safety temperature can be defined as the maximum temperature which initiates unsafe phenomena in the chemical reactor, usually referred to as the Maximum Allowable Temperature, MAT (Maestri and Rota, 2006).

3. Case study: Venturi loop ethoxylation reactor impinged by a vertical jet-fire

Ethoxylation is a polyaddition reaction of ethylene oxide (EO) to an alcohol (1-dodecanol in this case). This highly exothermic reaction (-92 kJ/mol) proceeds in liquid phase, after dissolution of EO from the gas phase. A decrease in the fluid density is observed at increasing degree of ethoxylation, while the solubility of EO is slightly affected by the ethoxylation degree (Di Serio et al., 2005). An undesired exothermic reaction is the EO decomposition to CH_4 and CO (-132 kJ/mol) at high temperatures in the gas phase (Crocco et al., 1959).
This process is usually carried out in dedicated reactors, where mass transfer is maximised in order to enhance the dissolution of EO in the reacting liquid. Moreover, such reactors involve a low fraction of EO in the gas phase to reduce flammability and decomposition problems. One of such reactors is the Venturi Loop Reactor (VLR) which adopts a liquid ejector to mix the reacting liquid while introducing EO by Venturi effect (Di Serio et al., 2005). The reactor is equipped with an external recirculation through a shell-and-tube heat exchanger to control the reaction exothermicity.
Nonetheless, the process is still intrinsically unsafe due to the exothermicity of both desired and undesired reactions, together with the increase in pressure due to decomposition and slightly by the increase in the liquid volume. A possible loss of thermal or pressure control can happen for example if the heat exchanger becomes inefficient in the removal of heat both because of internal (i.e., the reactions) or external (e.g., a fire) reasons.
As shown in Figure 1-a, the reactor is hemispherically capped and has a diameter of 1.5 m, with a total height equal to 6.5 m. The bottom of the reactor is at 1.5 m from the ground, while the external vertical pipe is 20 cm in diameter. The EO feed line is at 1.2 m from the ground and 25 cm from the main axis of the reactor. The reactor is initially charged with 1200 kg of 1-dodecanol under nitrogen atmosphere and fed with EO for 120 minutes at a rate of 1000 kg/h. Nitrogen is also fed (0.651 kg/h) as the EO storage tank is blanketed with nitrogen. The initial pressure is equal to 1.5 bar, and the initial temperature is equal to the coolant temperature (170 °C), which is maintained constant throughout the entire process. The product of heat exchange coefficient and area in the external heat exchanger is equal to 40,000 W/K. All the other physical and chemical data are taken from Di Serio et al. (2005).
The resulting geometry was reproduced in FDS as reported in Figure 1-b. The reactor has been described with 3D voxels of characteristic dimension equal to 5 cm, which was determined to be a sufficient resolution to properly describe the interaction between the fluid motion and the reactor obstruction.
The ethoxylation process presents several major risks related to the presence of the EO (Salzano et al., 2006). Among the others, in this work the accidental scenario involving a gaseous jet fire from the ethylene oxide feed line was investigated. In particular, a leak from an equivalent orifice of 1.5 cm of diameter (~1/3 of

pipe diameter) was assumed, leading to a flowrate of about 0.179 kg/s of EO. In the computational domain, the jet source was approximated by an area of 2.5x2.5 cm^2 as a compromise between computational effort and precision (Favrin et al., 2018).

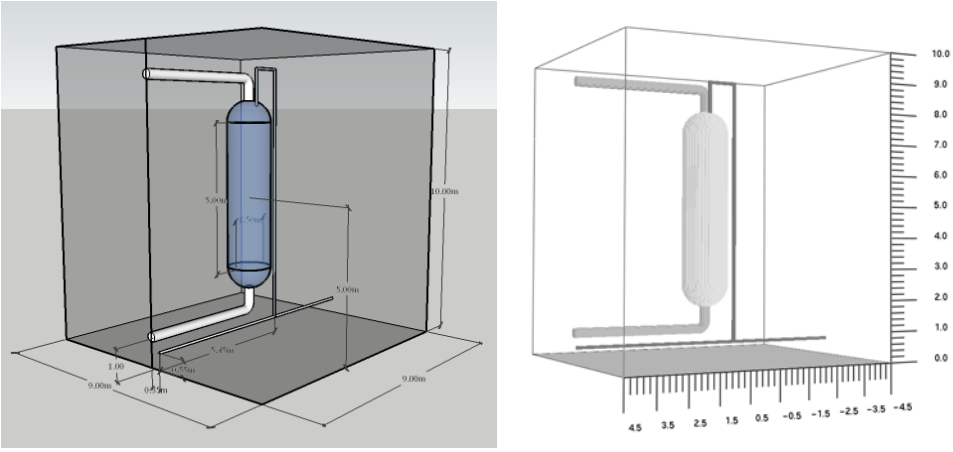

Figure 1: Side view with the characteristic dimensions of the reactor and corresponding FDS geometry.

3.1 CFD modelling of the jet-fire

The computational domain used in the CFD computation is 9x9x10 m, and it was meshed with cells ranging from 1.25 cm in the source region to 10 cm in the far field zone, resulting in about 10 million cells.
Boundary conditions of the domain where set as open surfaces with the exception of the ground which was assumed to be adiabatic. Reactor walls were assumed to be 6 mm thick made of stainless steel without insulation. Physical properties of stainless steel are reported in Table 1. The internal wall of the reactor was assumed to be at the process temperature, as the external surface at the beginning of the simulation.
The default combustion model of FDS was used, where the fuel was defined as EO with physical properties reported in Dorofeeva (1992). Particular attention has been payed to the influence of temperature on heat capacity and thermal conductivity, defined through linear interpolation of experimental data.

Table 1: Stainless steel properties.

-	Density $\left[\frac{kg}{m^3}\right]$	Specific Heat	$\left[\frac{kJ}{kg\,K}\right]$	Thermal conductivity	$\left[\frac{W}{m\,K}\right]$
	7850	0.45	at 20°C	48	at 20°C
		0.60	at 377°C	30	at 677°C
		0.85	at 677°C		

To calculate the net heat flow incoming in the reactor, four series of monitors were used. In particular, “Net Heat Flux” monitors, which register both the radiative and the convective contributions, were used. In Figure 2-a, the positions of the different groups (Xn, Xp, Yn, Yp) are reported. Each series consist in 30 monitors, distributed between the hemispherical bottom (14 monitors) and the cylindrical body (16 monitors) of the reactor. In order to take into account, the voxel discretization, in the hemispherical region the monitors number was doubled in seven positions to register both the horizontal and the vertical components of the heat flux for calculating the heat flux into the reactor.
This was carried out by assigning a portion of the surface to each monitor, assuming that the variation of the heat flux in the selected area is negligible, as:

$$\dot{q}_i = \hat{q}_i \, A \tag{1}$$

where $\dot{q}_i$ is the net heat flow entering from the i^{th} area A associated to the i^{th} monitor and $\hat{q}_i$ is the computed specific heat flux. In Figure 2-b a scheme of the computed components of the heat flux for a single monitor is reported. It is possible to notice that, depending on the position, different calculations are required to obtain the heat flux. In the cylindrical region of the reactor, only the horizontal component is considered, allowing the calculation as:

$\dot{q}_i = \hat{q}_i (2\ R\ \pi\ \delta h_i)/4$ *for all the sensors in the cylindrical region* (2)

where R is the radius of the reactor and δh_i is the height of the cylindrical area associated to the monitor. For each monitor in the cylindrical region the area is one fourth of the total, because at each height four sensors are equally distributed along the circumference of the reactor.

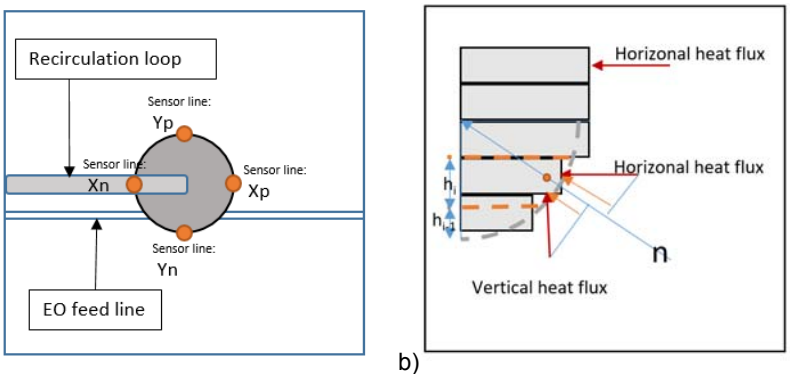

Figure 2: Positioning of monitors series on the Venturi loop reactor (a) and a scheme of the heat flux calculation performed (b).

Instead, in the hemispherical region, the coupling of two sensors (one vertical and one horizontal) allows to estimate the specific heat flux normal to the real surface of the reactor in that point:

$\hat{q}_i = \hat{q}_{i,vertical} \cdot \hat{n} + \hat{q}_{i,horizontal} \cdot \hat{n}$ *for all the sensors in the hemispherical region* (3)

where $\hat{n}$ is the normal to the surface in the point.
Once the normal specific heat flux was obtained, the heat flow for each i^{th} area is calculated as:

$\dot{q}_i = \hat{q}_i \left(2\ R\ \pi\ (h_i - \sum_{j=1}^{i} h_j\ )\right)/4$ (4)

As for the cylindrical region, the region associated to each monitor is one fourth of the circumference.
Finally, total heat flow is obtained as the sum of all the contributions:

$\dot{q}_{tot} = \sum_{i}^{n\ monitor} \dot{q}_i$ (5)

This approach allows to deal with the orthogonality of the geometry (imposed by the solver mesh) in a simple and effective way, being the error introduced by this simplification negligible.

3.2 0-D model of the reactor and runaway criteria

A mathematical model of the Venturi loop reactor can be developed from mass and energy balances. As the ejector guarantees a high degree of mixing, the reactor can be regarded as a perfectly mixed system, so the model becomes 0D. In particular, the mathematical model discussed in detail by Di Serio et al. (2005) was complemented by the energy balance and the EO decomposition reaction (Crocco et al., 1959).
The MAT was chosen equal to the critical temperature of EO (196 °C). The reason is that the solubility of EO decreases in the supercritical region, leading to an accumulation of EO in the gas phase. This favours EO decomposition, being this reaction of first order in EO (Crocco et al., 1959). Below the selected MAT, EO decomposition surely plays a marginal role in the build-up of pressure. On the contrary, when the reactor temperature becomes larger than that, not necessary EO decomposition plays a relevant role in the build-up of pressure. In other words, the assumed MAT value is expected to be quite conservative, which is a welcomed feature when highly hazardous materials like EO are involved.

4. Results

In this section, results obtained from the FDS simulation are presented together with the reactor behaviour predicted by the 0D model in the considered scenario.

4.1 CFD results

The results obtained from the CFD analysis allow to identify the more stressed area and the distribution of the heat flux, giving a comprehensive understanding of the fire effects on the reactor. An example of the monitors results is reported in Figure 3-a, where the computed specific heat flux is reported for the four series of sensors, at the same height from the bottom of the reactor (1.5 m), as a function of time. It can be noticed the large difference in the specific heat flux computed in the region impinged by the flame (about 75 kW/m^2) and the impinged (about 0 kW/m^2).
The main outcome from these CFD results, which is the input for the 0-D model, is the total heat flow entering the reactor, which is computed through equation (5) and reported in Figure 3-b. It is possible to see that the steady state results in a heat flow of about 600 kW and it is reached in less than 3 seconds, allowing to consider a constant value during the whole scenario.

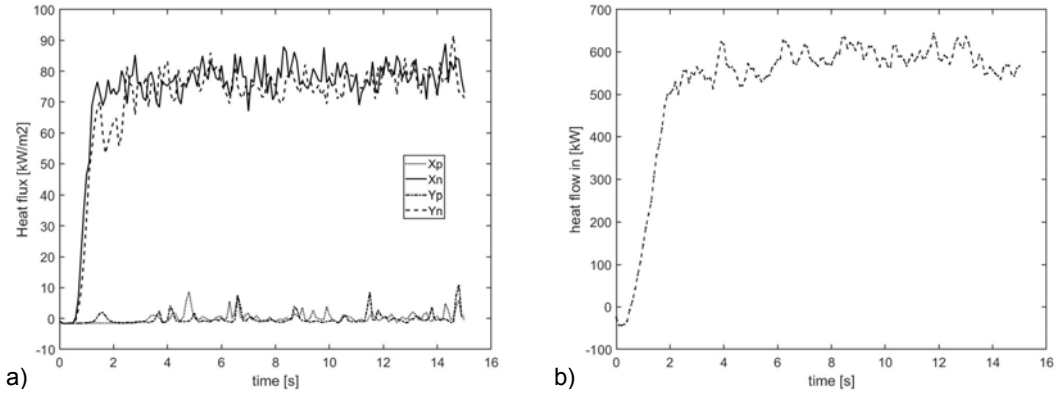

a) b)

Figure 3: Heat flux distribution at 1.5 m from the bottom of the reactor (a) and total heat flux entering the reactor (b).

4.2 0-D model results

According to the values of power input (which depends on the jet fire scenario), time at which the jet fire arises, and to the duration of the flame, the reactor can overcome the MAT value before the process is ended.
Figure 4-a displays three examples for the CFD simulated jet fire (600 kW). A and B accidental scenarios begin at the same time, but last for different times (see Figure 4-b). The shortest (B) does not lead to reach the MAT, while the longest (A) does. Another case, involving a flame that starts at a different initial time, but with the same duration as the one of case B, does not lead to overcome the MAT value neither.
Performing computations for different flame durations (which depend on the EO shutdown procedure and starting times of the flame) a boundary on the plane Flame duration vs Flame starting time can be identified, which separates a region where the MAT can be reached from a region where safe conditions are maintained. Figure 4-b depicts such regions. Note that the flame time is taken with respect to the beginning of the chemical process. In all analysed conditions, even when the MAT is overcome, the EO decomposition plays a marginal role. From Figure 4-b it is also possible to note that the worst case, happening close to the process end, involves a critical flame duration of 80 s. This calls for emergency shut-down procedures of EO, allowing to stop the EO loss in less than a minute.

5. Conclusions

In all the analysed scenarios the time required to reach the MAT can be lower than the flame duration, meaning that hazardous conditions can be always reached. However, the heat exchanger can provide enough cooling power to prevent dangerous conditions in short jet fire impingements (examples B and C of Figure 4).
Boundary maps such that depicted in Figure 4-b can allow to design efficient protection systems or to highlight criticalities. In the considered scenario, active countermeasures should be able to extinguish the jet fire in less than 80 s. As previously mentioned, the MAT value assumed for this analysis is quite conservative; however, similar boundary maps can be easily built by assuming different values for the MAT: similar conclusions would arise, with different values of the maximum allowable flame duration.

Finally, it should be stressed that this analysis faces only safety problems related to the temperature increase of the reactive mass. However, it is well known that other safety problems (mainly related to the structural integrity of the vessel/pipes) can arise from a jet-fire impingement scenario.

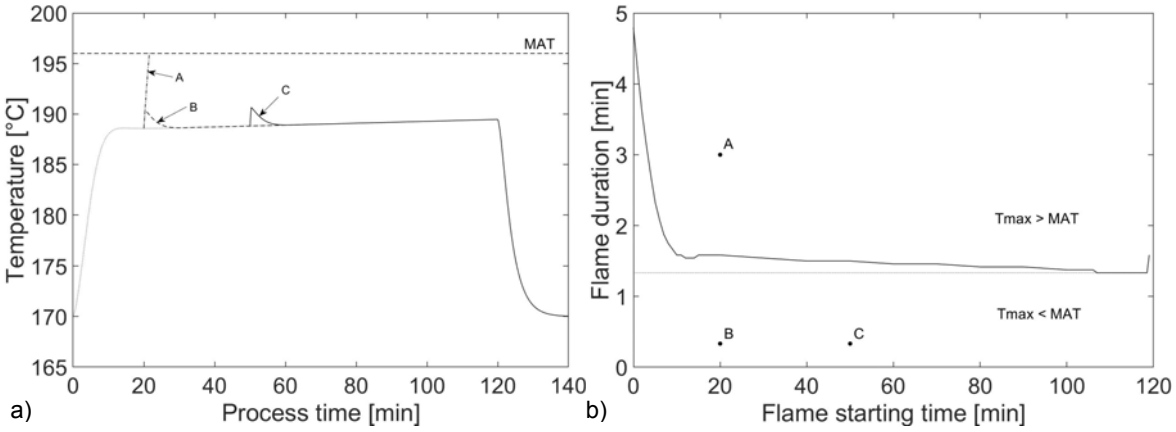

Figure 4: Behaviour of the reactor under flame impingement starting at different times during the chemical process: (a) Temperature profile in time for three scenarios: flames A and B start at 20 min, C at 50 min; A lasts for 3 min, while B and C for 20 s; (b) Runaway boundary.

References

Boot H., 2016, Developments in Modelling of Thermal Radiation from Pool and Jet Fires, Chemical Engineering Transactions, 48, 67 – 72.

Crocco L., Glassman I., Smith I. E., 1959, Kinetics and Mechanism of Ethylene Oxide Decomposition at High Temperatures, The Journal of Chemical Physics, 31, 506 – 510.

Chakrabarty A., Mannan S., Cagin T., 2015, Multiscale Modeling for Process Safety Applications, Butterworth-Heinemann, US.

Di Serio M., Tesser R., Santacesaria E., 2005, Comparison of Different Reactor Types Used in the Manufacture of Ethoxylated, Propoxylated Products, Ind. Eng. Chem. Res., 44, 9482 – 9489.

Dorofeeva O. V., 1992, Ideal gas thermodynamic properties of oxygen heterocyclic compounds. Part 1. Three-membered, four-membered and five-membered rings, Thermochim. Acta, 194, 9 – 46.

Maestri F., Rota R., 2006, Temperature diagrams for preventing decomposition or side reactions in liquid–liquid semibatch reactors, Chemical Engineering Science, 61, 3068 – 3078.

Maestri F., Rota R., 2016, Kinetic-Free Safe Operation of Fine Chemical Runaway Reactions: A General Criterion, Ind. Eng. Chem. Res., 55 (4), 925 – 933.

McGrattan K., Hostikka S., McDermott R., Floyd J., Weinschenk C., Overholt K., 2013, Fire Dynamics Simulator, Technical Reference Guide, Mathematical Model, vol. 1, NIST Special Publication 1018.

Favrin S., Busini V., Rota R., Derudi M., 2018, Practical LES Modelling of Jet Fires: Issues and Challenges, Chemical Engineering Transactions, 67, 259-264, DOI: 10.3303/CET1867044.

Reniers, G., Cozzani, V., 2013, Domino Effects in the Process Industries, 1st ed., Elsevier.

Sun L., Yan H., Liu S., Bai Y., 2017, Load characteristics in process modules of offshore platforms under jet fire: the numerical study, Journal of Loss Prevention in the Process Industries, 47, 29–40.

Salzano E., Di Serio M., Santacesaria E., 2007, The Evaluation of Risks of Ethoxylation Reactors, Process Safety Progress, 26, 304 – 311.

Salzano E., Di Serio M., Santacesaria E., 2007, The role of recirculation loop on the risk of ethoxylation processes, Journal of Loss Prevention in the Process Industries, 20, 238 – 250.

Tavelli S., Derudi M., Cuoci A., Frassoldati A., 2013, Numerical analysis of pool fire consequences in confined environments, Chemical Engineering Transactions, 31, 127 – 132.

Tavelli S., Rota R., Derudi M., 2014, A critical comparison between CFD and zone models for the consequence analysis of fires in congested environments, Chemical Engineering Transactions, 36, 247–252.